ACS APPLIED MATERIALS & INTERFACES

Research Article

www.acsami.org

One-Pot Synthesis of DNA-CdTe:Zn^{2+} Nanocrystals Using Na_2TeO_3 as the Te source

Cuiling Zhang, Ji Yan, Chen Liu, Xinghu Ji,* and Zhike He*

Key Laboratory of Analytical Chemistry for Biology and Medicine (Ministry of Education), College of Chemistry and Molecular Sciences, Wuhan University, Wuhan 430072, P. R. China

Supporting Information

ABSTRACT: DNA-functionalized quantum dots (QDs) are powerful tools for biosensing and bioimaging applications. Facile labeling methods with good fluorescence properties are desirable for the development of DNA-functionalized QDs. In this article, we describe a novel and simple approach that leads to the synthesis of DNA-functionalized CdTe:Zn^{2+} QDs in one step. It is the first time that DNA-functionalized QDs have been prepared using sodium tellurite as the tellurium source by a hydrothermal method. This approach will greatly reduce the synthesis time (only about 1 h) and simplify the synthesis process as well as reduce the complexity of the required experimental techniques. The as-prepared QDs exhibit high quantum yield, small size, and low toxicity. UV−vis spectra and FTIR characterization proved that the abundance of DNA on the surface of the QDs increased with the increase in the concentration of the feed DNA. Most importantly, these QDs functionalized with DNA have great potential to bind specifically to DNA, protein, and cell surface receptors.

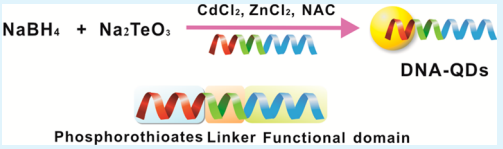

KEYWORDS: *DNA, Zn-doped quantum dots, Na_2TeO_3, one-step method, hydrothermal route*

INTRODUCTION

Semiconductor nanocrystals, which possess excellent optical properties and are incomparable relative to those of the traditional organic dyes, have received much attention in recent years.[1−4] Particularly, nucleic acid-functionalized nanocrystals play a crucial role in bioanalysis.[5−9] For such applications, high-fidelity nucleic acid functionalization of nanocrystals is desired and often obtained via electrostatic interaction, affinity binding (such as avidin−biotin binding), and covalent binding (mainly on amino/carboxy and metal ion/thiol groups).[10] These methods have certain advantages but also a few limitations.[11] A general approach to the synthesis of functionalized nanocrystals should be time- and labor-saving and inexpensive. Nucleic acids can serve as robust ligands for synthesis of semiconductor nanocrystals, and they can be used to tune the properties of nanocrystals.[12] The role of nucleic acids in nanocrystal growth is to passivate the nanocrystal surface, rendering the nanocrystals water-soluble and preventing agglomeration.[13] Additionally, the sequences and structures of nucleic acids can regulate the size, morphology, dispersity, emission maximum, and quantum yield of nanocrystals.

One-pot synthesis has been developed to prepare nucleic acids-functionalized CdTe nanocrystals that can be directly applied in biological targeting owing to the molecular-recognition capabilities of the designed nucleic acids.[14] Recently, our group has developed an interesting graphene-based DNA-functionalized CdTe nanocrystal probe by one-pot synthesis for the sensing of hepatitis B virus.[11] To improve the optical properties and to reduce the toxicity of DNA-functionalized nanocrystals to make them more suitable for biosensing and bioimaging applications, we previously developed an approach that leads to the synthesis of aptamer-functionalized CdTe:Zn^{2+} quantum dots through a facile one-pot hydrothermal route for tumor-targeted fluorescence imaging in vitro and in vivo.[15] The quantum dots exhibit small size, high quantum yield, and low toxicity. However, all of the above-mentioned protocols require inert conditions to obtain the precursor (NaHTe), and its injection is always uncontrollable.[16−18]

Herein, we devise a novel, one-step synthesis of DNA-functionalized CdTe:Zn^{2+} quantum dots (DNA-QDs) via a hydrothermal route in open air. Compared to the use of Te powder as the Te source in previous synthesis methods, sodium tellurite (Na_2TeO_3) was used herein, which is stable in air and has been utilized to prepare DNA-QDs in aqueous solution. The reaction can be accomplished in open air with a single step because Na_2TeO_3 can be easily reduced by sodium borohydride. In addition, the toxicity of the QDs has been greatly decreased because of the Zn-doping and DNA as the ligand.[15,19] The targeting QDs synthesized by this facile one-step method have a high quantum yield, small size, and low toxicity. All of these advantages make it possible for these QDs to be widely applied in biosensing and bioimaging.

EXPERIMENTAL SECTION

Chemicals and Apparatus. Na_2TeO_3 (99.999%), $CdCl_2·2.5H_2O$ (99%), $ZnCl_2$ (98%), and sodium borohydride ($NaBH_4$) were purchased from Shanghai Chemical Reagents Company. NAC

Received: October 9, 2013
Accepted: February 10, 2014
Published: February 10, 2014

   dx.doi.org/10.1021/am405864z | ACS Appl. Mater. Interfaces 2014, 6, 3189−3194

(98%), rhodamine B, and rhodamine 6G were obtained from Sigma. All chemicals were used without additional purification. All solutions were prepared using Milli-Q water (Millipore) as the solvent. Modified DNA 5′-CCTGGTGCCGTAGATAAAAAAG*G*G*G*G*G*G*G*-G*G*G*-3′ (* indicates the phosphorothioate linkage) was synthesized by Shanghai Sangon Biotechnology Co. Ltd. (China).

Vero cells were cultured in Dulbecco's modified Eagle's Medium (DMEM) containing 10% fetal bovine serum (FBS). UV−vis absorption spectra were obtained using a Shimadzu UV-2550 spectrophotometer (Japan). Fluorescence spectra were collected on a Shimadzu RF-5301 spectrofluorometer. All optical measurements were performed at room temperature under ambient conditions. X-ray diffraction (XRD) patterns were obtained using a Bruker D8 Discover X-ray diffractometer (German). X-ray photoelectron spectroscopy (XPS) was carried out using a Kratos Ltd. Xsam-800 X-ray photoelectron spectrometer (UK). Atomic absorption spectrometry (AAS) measurements were measured on a PerkinElmer Analyst 80 atomic absorption spectrometer (USA). Transmission electron microscopy (TEM) and high-resolution (HR) TEM images were recorded on a JEOL Ltd. JEM 2100 electron microscope (Japan). The CCK-8 assay was acquired with a microplate reader (Bio-Rad550, USA).

Synthesis of DNA-QDs. The preparation of DNA-QDs by a one-step hydrothermal route using Na_2TeO_3 as the Te source was carried out as follows. In a typical procedure, $CdCl_2·2.5H_2O$ (6.25 mM), $ZnCl_2$, and NAC were dissolved in deionized water at a molar ratio of 1:1:1.2. The pH of the solution was adjusted to 8.0 with a 1.0 M NaOH solution. Then, $NaBH_4$ (1.25 mM) and Na_2TeO_3 (3.125 mM) were added to the mixture solution under vigorous stirring. After 5 min, different concentrations of DNA solution were added to the mixture solution. Last, the mixture was moved to a Teflon-lined stainless steel autoclave. The reaction was carried out at 200 °C for different amounts of time (from 26 to 38 min). The solution was cooled to the room temperature. Next, the product was obtained by ultrafiltration using an Amicon Ultra-4 centrifugal filter device with a MW cutoff of 30 kDa (Millipore Corp.) The concentrated product was then lyophilized to obtain the final product, which was used for XRD and FTIR analysis. Quantum yields were measured using rhodamine 6G and rhodamine B (Sigma) in ethanol as the reference standard (QY = 95 and 98%, respectively).[20]

Measurement of Cytotoxicity. Cytotoxicity of DNA-QDs was assessed using the CCK8 (Dojindo Laboratories, Tokyo, Japan) to count Vero cells. Briefly, Vero cells (1.0×10^4 cells/well) were seeded into 96-well plates in 100 μL of DMEM. After 24 h at 37 °C, DNA-QDs were added into each well, and the plates were incubated for 24 h. Ninety microliters of fresh DMEM was used to replace the supernatant, 10 μL of CCK-8 solution was added to each well of the plates, and the plates were incubated for 2 h in the incubator (37 °C and 5% CO_2). The absorbance was measured with a microplate reader at 450 nm.

RESULTS AND DISCUSSION

Scheme 1 depicts the synthetic route for the DNA-QDs. In the traditional method (Scheme 1A), NaHTe serves as the Te source and is obtained from the Te power. The reaction of Te power and $NaBH_4$ is usually carried out in an ice bath for a few hours only in the absence of oxygen. In addition, controlling the transfer process of the NaHTe product requires good technicians. In this research, Na_2TeO_3 was used for the first time to synthesize DNA-QDs by a one-step method (Scheme 1B). *N*-Acetyl-L-cysteine (NAC)[21,22] and a specific DNA[11,14,15] sequence were employed as the coligand to prepare the QDs. Zinc was also doped in the synthesis process. Compared to the previous method, this approach drastically shortens the time, only requiring about 1 h. At the same time, the necessity for skilled researcher is also greatly reduced. All of these factors have helped to improve the scale of the preparation.

Scheme 1. Schematic Representation of DNA-QDs Synthesis[a]

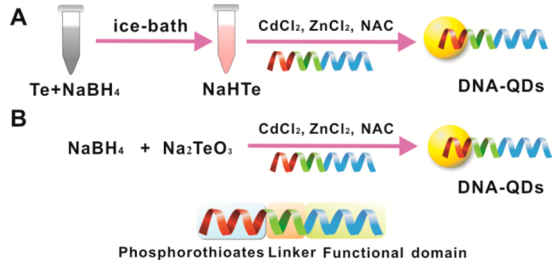

[a](A) Traditional preparation method of the DNA-QDs using Te power as the tellurium source and (B) novel preparation method of DNA-QDs using Na_2TeO_3 as the tellurium source.

Preparation of CdTe:Zn^{2+} QDs. CdTe:Zn^{2+} QDs using Na_2TeO_3 as the Te resource were prepared. As is known, the ratio of various precursors can greatly affect the fluorescence qualities of the prepared QDs. We performed a series of experiments to determine the optimum pH (Figure S1A) and the ratio of various precursors including $CdCl_2/Na_2TeO_3$ (Figure S1B) and $NaBH_4/Na_2TeO_3$ (Figure S1C). The influence of different Zn/Cd ratios is displayed in Table 1

Table 1. Relation between Feed Ratio (FR) and Actual Constituent Ratio (ACR) of Cd/Zn and the Optical Properties of CdTe:Zn^{2+} QDs

$FR_{n(Cd):n(Zn)}$	λ_{em} (nm)	FWHM (nm)	QY (%)	$ACR_{n(Cd):n(Zn)}$
1:0	533	37	42.0	1:0
1:0.5	535	37	56.6	1:0.13
1:1	536	35	59.9	1:0.2
1:2	534	35	53.8	1:0.26
1:3	535	35	50.0	1:0.3

and is similar to our previous report.[21] Under the same reaction conditions, the quantum yields (QY) were much improved and the FWHM slightly decreased as the ratio of Zn increased. The difference is because of the influence of the Zn/Cd ratio on the QY of the QDs. When the feed ratio of Zn/Cd reached 1:1, the actual constituent ratio in the prepared QDs was 1:0.2 and the QY was the highest. The most likely reason for this is that Zn was consumed by side reactions.

Preparation of DNA-CdTe:Zn^{2+} QDs. DNA-QDs were synthesized by a one-step method. In the synthesis process, DNA as the coligand was added under optimized conditions for CdTe:Zn^{2+} QDs. We obtained the UV−vis absorption and fluorescence spectra of a series of as-prepared DNA-QDs with controllable maximum emission wavelength ranging from 538 to 616 nm in aqueous solution (Figure 1). As the reaction time was increased, the emission wavelength was red-shifted, the FWHM was gradually widened, and the QY could be as high as 73.9% (Table 2). Combining data from Table 1 with that from Table 2, it can be seen that the QY of the DNA-QDs is higher than that of QDs, demonstrating that DNA as the coligand can passivate the QDs surface and lead to a better crystal lattice.[13,23] The actual Zn/Cd ratio in the prepared DNA-QDs was 1:0.2 by AAS. In short, the DNA-QDs possess good fluorescence characteristics.

Availability of the Modifying DNA on QDs. The availability of the modifying DNA for hybridizing the complementary DNA was tested using SYBR green 1

dx.doi.org/10.1021/am405864z | ACS Appl. Mater. Interfaces 2014, 6, 3189−3194

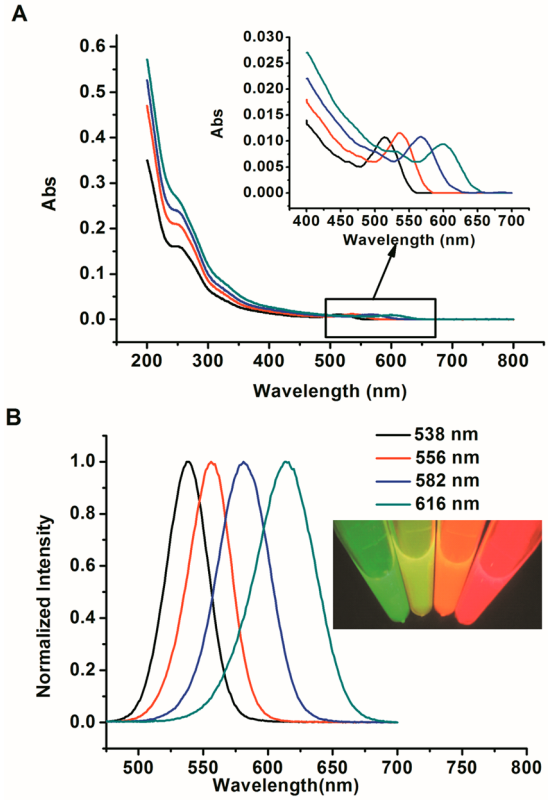

Figure 1. Series of (A) UV–vis and (B) fluorescence spectra of the DNA-QDs with maximum emission wavelengths ranging from 538 to 616 nm. The photograph in the inset in panel B is a DNA-QDs aqueous solution under UV irradiation.

Table 2. Optical Properties of DNA-QDs Obtained at Various Reaction Times

reaction time (min)	λ_{em} (nm)	FWHM (nm)	QY (%)
26	538	37	66.7
30	556	38	73.9
34	582	46	56.8
38	616	53	59.8

intercalative dye (Figure S2). SYBR green 1 binds to double-stranded DNA, and the fluorescence of SYBR green 1 significantly enhances. In this method, the added complementary DNA could form the dsDNA with the DNA-QDs, thus the fluorescence of SYBR green 1 was increased sharply when it was added. This result suggested the availability of the modifying DNA.

Influence of the Amount of DNA on the DNA-QDs. Different amounts of DNA (10–120 nmol) were added during the synthesis process, and the UV–vis spectra of these QDs were measured, as shown in Figure 2A. The ultraviolet absorption peaks at 260 nm were gradually increased, which indicates that the amount of DNA molecules on the QD surface increased. The quantitative loading of DNA on the QDs was calculated as ca. 0.13, 0.88, 1.58, 2.76, and 4.45 (amount of DNA from 10 to 120 nmol) according to the absorption spectra of the QDs (data not shown) and DNA-QDs. This result is also corroborated by Fourier transform infrared spectroscopy (FTIR), which can provide insight into the chemical nature of the DNA capping. Figure 2B presents the FTIR of DNA-QDs, where differences are observed with the

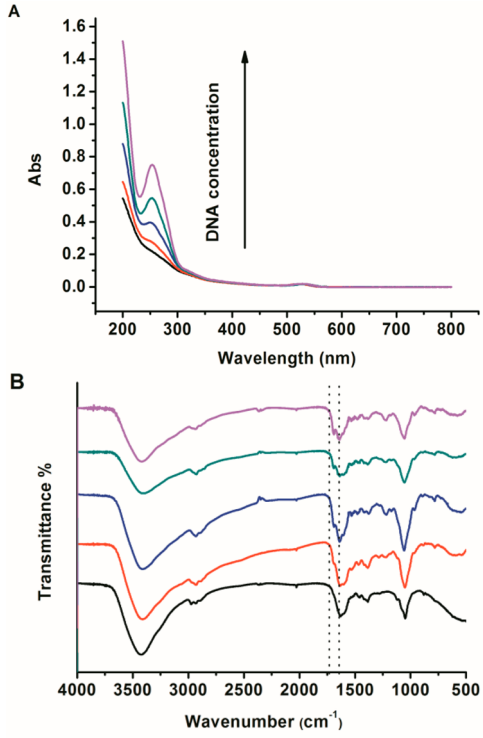

Figure 2. (A) UV–vis absorption spectra of DNA-QDs with different amounts of DNA (10, 20, 40, 80, 120 nmol from bottom to top). (B) FTIR spectra of DNA (10, 20, 40, 80, 120 nmol from bottom to top) bound to QDs.

increase in the amount of DNA. The obvious difference is mainly demonstrated from the peak at 1690 cm^{-1}, which corresponds to C6═O6 stretching, N1–H bending, or $-NH_2$ scissoring of guanine.[24,25] In addition, the value of the peak increased with the increase in the amount of DNA molecules on the QDs.

Characterization of DNA-QDs. The transmission electron microscopy (TEM) image reveals that DNA-QDs (λ_{em} = 556 nm) are spherical particles with good monodispersibility (Figure 3A) and an average size of 3.5 ± 0.3 nm (Figure 3B). The small size is advantageous for their use in bioimaging compared with the traditional DNA-functionalized QDs produced by the bridge of biotin and avidin, which result in larger sizes that can bind to all biotinylated proteins in the sample and may lead to aggregate formation.[26] The inset in Figure 3A is the high-resolution TEM (HRTEM) image of DNA-QDs, which shows its high crystallinity. The powder X-ray diffraction (XRD) pattern of DNA-QDs is displayed in Figure 3C. The positions of the diffraction peaks at wide angles match those of the cubic structure of CdTe quantum dots (zinc blende structure). X-ray photoelectron spectroscopy (XPS), which is a typical surface analytical tool, was used to analyze the surface chemical compositions of the DNA-QDs, QDs, and CdTe. Figures 3D and S4A show the overview spectra of the DNA-QDs and QDs, respectively. The characteristic Zn (2p) peaks at 1020.1 and 1043.1 eV[27] are in the inset of Figure 3D. This is direct evidence that Zn exists in DNA-QDs. Figure S4B displays the Zn peaks of QDs at 1020.2 and 1043.3 eV, which were almost the same values as the Zn peaks of DNA-QDs, revealing that DNA as the coligand does not influence the surface structure of the QDs. The XPS spectrum of CdTe is also provided in Figure S5A. Additionally, the typical

dx.doi.org/10.1021/am405864z | ACS Appl. Mater. Interfaces 2014, 6, 3189–3194

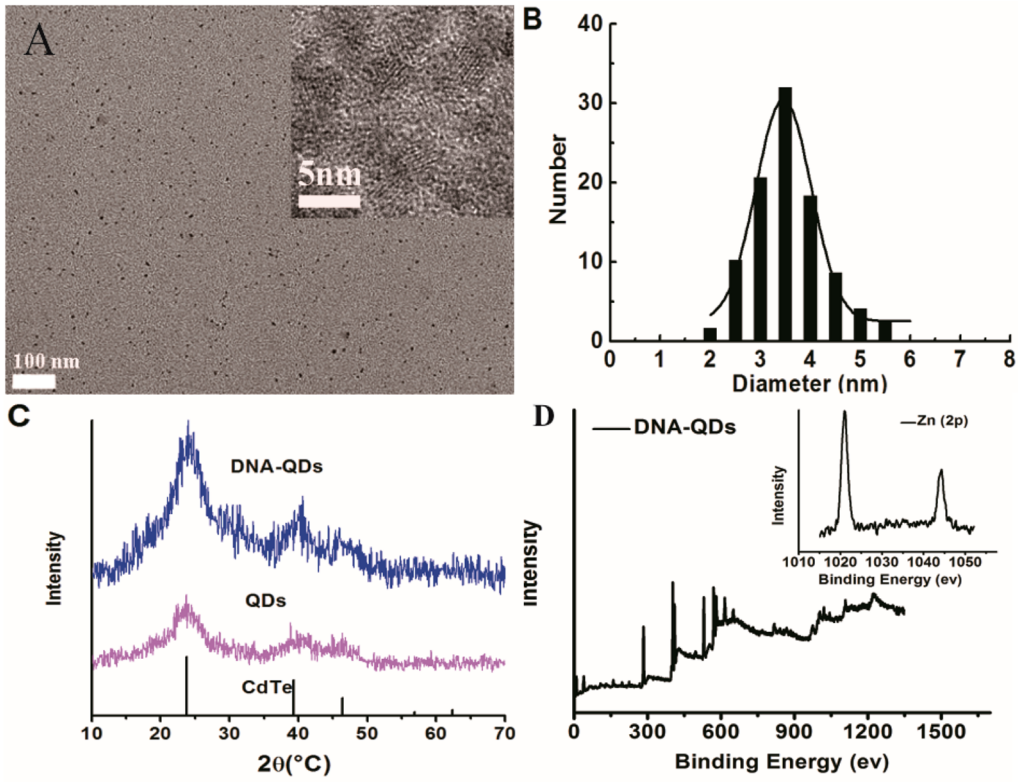

Figure 3. (A) TEM images of DNA-QDs (λ_{em} = 556 nm). Inset: HRTEM image. (B) Size distribution of DNA-QDs. (C) XRD patterns of DNA-QDs (blue line) and QDs (violet line) in comparison to the standard pattern of cubic phase (JCPDS card 15-0770) of CdTe (blank line). (D) XPS spectrum of DNA-QDs. Inset: narrow-scan XPS spectrum of Zn (2p) recorded from DNA-QDs.

characteristic peaks of Cd (3d) of the DNA-QDs, QDs, and CdTe are shown in Figures S3, S4C, and S5B.

Photostability of DNA-QDs and CdTe. The photostabilities of the prepared DNA-QDs and CdTe were evaluated using a 150 W xenon lamp at 350 nm for 1 h (Figure 4). The

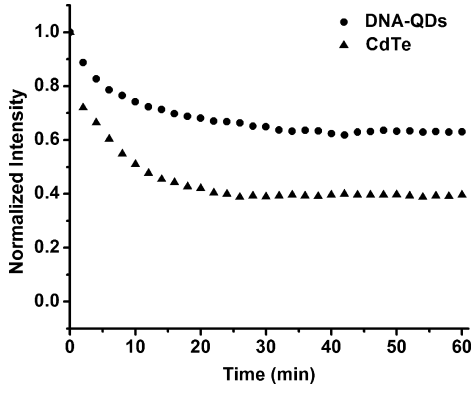

Figure 4. Photostability of DNA-QDs (●) and CdTe (▲).

emission intensities of both DNA-QDs and CdTe were approximately stabilized within 30 min. It should be noted that the intensity of CdTe dropped rapidly in the first 30 min; the DNA-QDs had a slow decrease in intensity. The intensity of the DNA-QDs stabilized at about 69%, whereas the CdTe stabilized with only 40% left. In essence, the DNA-QDs possess better performance than CdTe.

Cytotoxicity Assay. The cytotoxicity of DNA-QDs is critically important for biological systems. As we have described in previous reports, the cytotoxicity of cadmium-based quantum dots is very drastic.[28−33] The reason for this is mainly because of the release of free Cd^{2+} ions from the quantum dots surface and the stability of the QD surface coating. Here, because of the Zn-doping and the use of DNA as a surface coligand, it seemed likely that Cd^{2+} ions and ligand-induced toxicity could be greatly reduced. This supposition was proved in our previous study.[15] Compared to QDs (CdTe:Zn^{2+} QDs) and CdTe QDs, DNA-QDs have the lowest toxicity and CdTe QDs are the most toxic. The toxicity of DNA-QDs and QDs were examined using Vero cells (kidney epithelial cells) (Figure 5). As expected, the toxicity of QDs is higher than that from DNA-QDs because of the use of DNA as coligand. No appreciable loss in cellular viability with DNA-QDs was

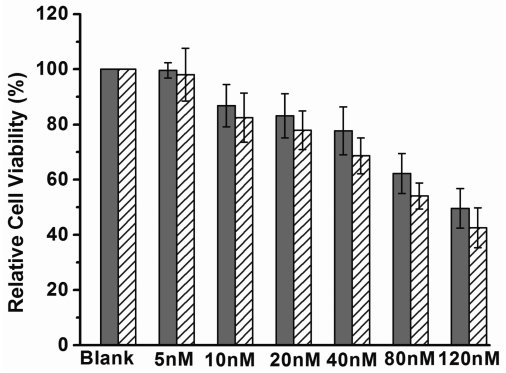

Figure 5. Cell viability data for DNA-QDs and QDs. Vero cells were incubated with different concentrations of DNA-QDs and QDs (5, 10, 20, 40, 80, and 120 nM) for 24 h, and cytotoxicity was measured using the CCK-8 assay.

observed using a Cell Counting Kit-8 (CCK-8) assay when 5 nM DNA-QDs was added, and the cellular viability of Vero cells was almost 80% with 40 nM DNA-QDs. This dose is enough to meet requirements in bioimaging. When the concentration of DNA-QDs is 120 nM, there is still about 50% cellular viability. This observation suggests that the as-prepared DNA-QDs can be considered as having low toxicity, making them biocompatible for biological applications.

CONCLUSIONS

DNA-functionalized CdTe:Zn^{2+} quantum dots using Na_2TeO_3 as the Te source were directly prepared in aqueous solution through a facile one-step hydrothermal synthesis. The QDs display small size, low toxicity, excellent biocompatibility, and good optical properties. This approach will greatly reduce the synthesis time (only about 1 h) and simplify the synthesis process as well as reduce the complexity of the required experimental techniques. In addition, the QDs with target DNA have the potential to bind specifically to DNA, protein, and cell surface receptors. These unprecedented advantages may make the QDs a promising tool for use in biological sensing and imaging.

ASSOCIATED CONTENT

Supporting Information

Effects of various precursors on QDs and XPS of CdTe:Zn^{2+} QDs and CdTe. This material is available free of charge via the Internet at http://pubs.acs.org.

AUTHOR INFORMATION

Corresponding Author

*E-mail: zhkhe@whu.edu.cn. (Z.H.).

Author Contributions

The manuscript was written through contributions of all authors. All authors have given approval to the final version of the manuscript.

Notes

The authors declare no competing financial interest.

ACKNOWLEDGMENTS

This work was financially supported by the National Key Scientific Program Nanoscience and Nanotechnology (2011CB933600), the Suzhou Nanotechnology Special Project (ZXG2013028), the National Science Foundation of China (21275109), and the academic award for excellent Ph.D. candidates funded by the Ministry of Education of China (5052012203001).

REFERENCES

(1) Bruchez, M.; Moronne, M.; Gin, P.; Weiss, S.; Alivisatos, A. P. Semiconductor Nanocrystals as Fluorescent Biological Labels. *Science* **1998**, *281*, 2013−2016.

(2) Chan, W. C. W.; Nie, S. M. Quantum Dot Bioconjugates for Ultrasensitive Nonisotopic Detection. *Science* **1998**, *281*, 2016−2018.

(3) Resch-Genger, U.; Grabolle, M.; Cavaliere-Jaricot, S.; Nitschke, R.; Nann, T. Quantum Dots versus Organic Dyes as Fluorescent Labels. *Nat. Methods* **2008**, *5*, 763−775.

(4) Clapp, A. R.; Medintz, I. L.; Mauro, J. M.; Fisher, B. R.; Bawendi, M. G.; Mattoussi, H. Fluorescence Resonance Energy Transfer between Quantum Dot Donors and Dye-Labeled Protein Acceptors. *J. Am. Chem. Soc.* **2004**, *126*, 301−310.

(5) Freeman, R.; Finder, T.; Willner, I. Multiplexed Analysis of Hg^{2+} and Ag^{+} Ions by Nucleic Acid Functionalized CdSe/ZnS Quantum Dots and Their Use for Logic Gate Operations. *Angew. Chem., Int. Ed.* **2009**, *48*, 7818−7821.

(6) Gill, R.; Zayats, M.; Willner, I. Semiconductor Quantum Dots for Bioanalysis. *Angew. Chem., Int. Ed.* **2008**, *47*, 7602−7625.

(7) Freeman, R.; Liu, X. Q.; Willner, I. Amplified Multiplexed Analysis of DNA by the Exonuclease III-Catalyzed Regeneration of the Target DNA in the Presence of Functionalized Semiconductor Quantum Dots. *Nano Lett.* **2011**, *11*, 4456−4461.

(8) Sharon, E.; Freeman, R.; Willner, I. CdSe/ZnS Quantum Dots-G-Quadruplex/Hemin Hybrids as Optical DNA Sensors and Aptasensors. *Anal. Chem.* **2010**, *82*, 7073−7077.

(9) Freeman, R.; Girsh, J.; Willner, I. Nucleic Acid/Quantum Dots (QDs) Hybrid Systems for Optical and Photoelectrochemical Sensing. *ACS Appl. Mater. Interfaces* **2013**, *5*, 2815−2834.

(10) Frasco, M. F.; Chaniotakis, N. Bioconjugated Quantum Dots as Fluorescent Probes for Bioanalytical Applications. *Anal. Bioanal. Chem.* **2009**, *396*, 229−240.

(11) Zhang, C. L.; Xu, J.; Zhang, S. M.; Ji, X. H.; He, Z. K. One-Pot Synthesized DNA−CdTe Quantum Dots Applied in a Biosensor for the Detection of Sequence-Specific Oligonucleotides. *Chem.—Eur. J.* **2012**, *18*, 8296−8300.

(12) Hinds, S.; Taft, B. J.; Levina, L.; Sukhovatkin, V.; Dooley, C. J.; Roy, M. D.; MacNeil, D. D.; Sargent, E. H.; Kelley, S. O. Nucleotide-Directed Growth of Semiconductor Nanocrystals. *J. Am. Chem. Soc.* **2006**, *128*, 64−65.

(13) Ma, N.; Kelley, S. O. DNA-Based Programing of Quantum Dot Properties. *WIRES Nanomed. Nanobiotechnol.* **2013**, *5*, 86−95.

(14) Ma, N.; Sargent, E. H.; Kelley, S. O. One-Step DNA-Programmed Growth of Luminescent and Biofunctionalized Nanocrystals. *Nat. Nanotechnol.* **2009**, *4*, 121−125.

(15) Zhang, C. L.; Ji, X. H.; Zhang, Y.; Zhou, G. H.; Ke, X. L.; Wang, H. Z.; Tinnefeld, P.; He, Z. K. One-Pot Synthesized Aptamer-Functionalized CdTe:Zn^{2+} Quantum Dots for Tumor-Targeted Fluorescence Imaging in Vitro and in Vivo. *Anal. Chem.* **2013**, *85*, 5843−5849.

(16) Wu, P.; Li, Y.; Yan, X. P. CdTe Quantum Dots (QDs) Based Kinetic Discrimination of Fe^{2+} and Fe^{3+}, and CdTe QDs-Fenton Hybrid System for Sensitive Photoluminescent Detection of Fe^{2+}. *Anal. Chem.* **2009**, *81*, 6252−6257.

(17) Rajh, T.; Micic, O. I.; Nozik, A. J. Synthesis and Characterization of Surface-Modified Colloidal Cadmium Telluride Quantum Dots. *J. Phys. Chem.* **1993**, *97*, 11999−12003.

(18) Zheng, Y. G.; Gao, S. J.; Ying, J. Y. Synthesis and Cell-Imaging Applications of Glutathione-Capped CdTe Quantum Dots. *Adv. Mater.* **2007**, *19*, 376−380.

(19) Ma, N.; Yang, J.; Stewart, K. M.; Kelley, S. O. DNA-Passivated CdS Nanocrystals: Luminescence, Bioimaging, and Toxicity Profiles. *Langmuir* **2007**, *23*, 12783−12787.

(20) Grabolle, M.; Spieles, M.; Lesnyak, V.; Gaponik, N.; Eychmüller, A.; Resch-Genger, U. Determination of the Fluorescence Quantum Yield of Quantum Dots: Suitable Procedures and Achievable Uncertainties. *Anal. Chem.* **2009**, *81*, 6285−6294.

(21) Zhao, D.; Fang, Y.; Wang, H. Y.; He, Z. Synthesis and Characterization of High-Quality Water-Soluble CdTe:Zn^{2+} Quantum Dots Capped by N-Acetyl-L-cysteine via Hydrothermal Method. *J. Mater. Chem.* **2011**, *21*, 13365−13370.

(22) Zhao, D.; He, Z. K.; Chan, P. S.; Wong, R. N. S.; Mak, N. K.; Lee, A. W. M.; Chan, W. H. NAC-Capped Quantum Dot as Nuclear Staining Agent for Living Cells via an in Vivo Steering Strategy. *J. Phys. Chem. C* **2010**, *114*, 6216−6221.

(23) Ma, N.; Tikhomirov, G.; Kelley, S. O. Nucleic Acid-Passivated Semiconductor Nanocrystals: Biomolecular Templating of Form and Function. *Acc. Chem. Res.* **2009**, *43*, 173−180.

(24) Cha, T.-G.; Baker, B. A.; Salgado, J.; Bates, C. J.; Chen, K. H.; Chang, A. C.; Akatay, M. C.; Han, J.-H.; Strano, M. S.; Choi, J. H. Understanding Oligonucleotide-Templated Nanocrystals: Growth Mechanisms and Surface Properties. *ACS Nano* **2012**, *6*, 8136−8143.

(25) Mondragon-Sanchez, J. A.; Liquier, J.; Shafer, R. H.; Taillandier, E. Tetraplex Structure Formation in the Thrombin-Binding DNA

Aptamer by Metal Cations Measured by Vibrational Spectroscopy. *J. Biomol. Struct. Dyn.* **2004**, *22*, 365−373.
(26) Medintz, I. L.; Uyeda, H. T.; Goldman, E. R.; Mattoussi, H. Quantum Dot Bioconjugates for Imaging, Labelling and Sensing. *Nat. Mater.* **2005**, *4*, 435−446.
(27) Wagner, C. D.; Muilenberg, G. E. *Handbook of X-ray Photoelectron Spectroscopy*; Perkin-Elmer: Eden Prairie, MN, 1979.
(28) Derfus, A. M.; Chan, W. C. W.; Bhatia, S. N. Probing the Cytotoxicity of Semiconductor Quantum Dots. *Nano Lett.* **2004**, *4*, 11−18.
(29) Kirchner, C.; Liedl, T.; Kudera, S.; Pellegrino, T.; Muñoz Javier, A.; Gaub, H. E.; Stölzle, S.; Fertig, N.; Parak, W. J. Cytotoxicity of Colloidal CdSe and CdSe/ZnS Nanoparticles. *Nano Lett.* **2005**, *5*, 331−338.
(30) Chang, E.; Thekkek, N.; Yu, W. W.; Colvin, V. L.; Drezek, R. Evaluation of Quantum Dot Cytotoxicity Based on Intracellular Uptake. *Small* **2006**, *2*, 1412−1417.
(31) Su, Y. Y.; Hu, M.; Fan, C. H.; He, Y.; Li, Q. N.; Li, W. X.; Wang, L. H.; Shen, P. P.; Huang, Q. The Cytotoxicity of CdTe Quantum Dots and the Relative Contributions from Released Cadmium Ions and Nanoparticle Properties. *Biomaterials* **2010**, *31*, 4829−4834.
(32) Chen, N.; He, Y.; Su, Y. Y.; Li, X. M.; Huang, Q.; Wang, H. F.; Zhang, X. Z.; Tai, R. Z.; Fan, C. H. The Cytotoxicity of Cadmium-Based Quantum Dots. *Biomaterials* **2012**, *33*, 1238−1244.
(33) Wang, Y.; Hu, R.; Lin, G.; Roy, I.; Yong, K.-T. Functionalized Quantum Dots for Biosensing and Bioimaging and Concerns on Toxicity. *ACS Appl. Mater. Interfaces* **2013**, *5*, 2786−2799.